Bioorganic Chemistry 87 (2019) 474–483

Contents lists available at ScienceDirect

Bioorganic Chemistry

journal homepage: www.elsevier.com/locate/bioorg

Semi-synthetic isoflavones as BACE-1 inhibitors against Alzheimer's disease

Giovanni Ribaudo[a,1], Paolo Coghi[b,1], Enrico Zanforlin[a,1], Betty Yuen Kwan Law[b], Yuki Yu Jun Wu[b], Yu Han[b], Alena Congling Qiu[b], Yuan Qing Qu[b], Giuseppe Zagotto[a,*], Vincent Kam Wai Wong[b,*]

[a] Department of Pharmaceutical and Pharmacological Sciences, University of Padova, Via Marzolo 5, 35131 Padova, Italy
[b] State Key Laboratory of Quality Research in Chinese Medicine, Macau University of Science and Technology, Avenida Wai Long, Taipa, Macau

ARTICLE INFO

Keywords:
β-Secretase(BACE-1)
Isoflavones
P-gp
In silico molecular docking
Alzheimer's disease

ABSTRACT

BACE-1 is considered to be one of the targets for prevention and treatment of Alzheimer's disease (AD). We here report a novel class of semi-synthetic derivatives of prenylated isoflavones, obtained from the derivatization of natural flavonoids from Maclura pomifera. In vitro anti-AD effect of the synthesized compounds were evaluated via human recombinant BACE-1 inhibition assay. Compound **7**, **8** and **13** were found to be the most active candidates which demonstrates good correlation between the computational docking and pharmacokinetic predictions. Moreover, cytotoxic studies demonstrated that the compounds are not toxic against normal and cancer cell lines. Among these three compounds, compound **7** enhance the activity of P-glycoprotein (P-gp) on A549 cancer cells and increases the activity of P-gp ATPase with a possible role on the efflux of amyloid-β across the blood- brain barrier. In conclusion, the present findings may pave the way for the discovery of a novel class of compounds to prevent and/or treat AD.

1. Introduction

Alzheimer's disease (AD) is a devastating, progressive neurodegenerative disease that is associated with up to 80% of the estimated 47 million cases of dementia worldwide, and is one of the leading causes of death in the United States [1a,1b]. While there is no cure for AD [1c], there are 5 prescriptions drugs currently approved by food and drug administration (FDA) to treat its symptoms. Among them Donepezil, Galantamine and Rivastigmine are acetylcholinesterase (AChE) inhibitors (Fig. 1a), while Memantine is N–methyl-D-aspartate receptor antagonist (NMDA) (Fig. 1b) [1d].

The majority of developed drugs in the last 20 years were molecules interfering with aggregation of the β-amyloid (Aβ) peptide. In 1991 Aβ accumulation was initially proposed [2a–2c] as the main event of AD, while amyloid cascade hypothesis was proposed one year later [2d] and in course of years has evolved [2e]. BACE-1 is emerged as an important drug target for reducing Aβ levels in the AD and the development of BACE-1 inhibitors as therapeutic agents was pursed [2f]. BACE1 is the β-secretase enzyme cleaving the APP protein to release the C99 fragment that gives rise to various species of Aβ peptide during subsequent γ-secretase cleavage [2g].

Animal studies have indicated that prolonged treatment with some BACE1 inhibitors may negatively affect spine formation and density, hippocampal long-term potentiation, and cognition in wild-type mice [3]. A significant number of BACE inhibitors were abandoned because of poor tolerability and efficacy in man: Verubecestat (MK-8931, Merck) [4a], Lanabecestat (AZD-3293, LY3314814 Astra Zeneca and Eli Lilly) [4b], Atabecestat (JNJ-54,861,911, Janssen) [4c] showed recently problems and their trials were discontinued. Studies with derivative Elenbecestat [4d] and others [4e,4f] are ongoing and positive results on phase II/III were recently published. Therefore although drug discovery targeting the beta-amyloid remains controversial also recent studies [4g] on multi-target directed ligands has provided insight and hope on the use of natural products in targeting AD via BACE-beta amyloid mechanism. On the other hand, P-glycoprotein (P-gp) is a protein involved in the active transport of molecules across biological membranes, and it has been shown that alterations of its expression and/or activity are related to the onset of neurodegenerative disorders. Indeed, it has been reported that up-regulation of this ATP-dependent dependent efflux pump is necessary for a decrease of Aβ intracellular accumulation [5], suggesting the possible therapeutic approach for AD by activation of P-gp activity.

Recently, natural and semi-synthetic compounds captivated the interest of medicinal chemists, as they may represent promising and

* Corresponding authors. Tel.: +39-049-827-5686; fax: +39-049-827-5366 (G. Zagotto); Tel.: +853-8897 2408; fax: +853-2882 2799 (V.K.W. Wong).
E-mail addresses: giuseppe.zagotto@unipd.it (G. Zagotto), bowaiong@gmail.com (V.K.W. Wong).
[1] These authors contributed equally to this work.

https://doi.org/10.1016/j.bioorg.2019.03.034
Received 30 January 2019; Received in revised form 3 March 2019; Accepted 14 March 2019
Available online 15 March 2019

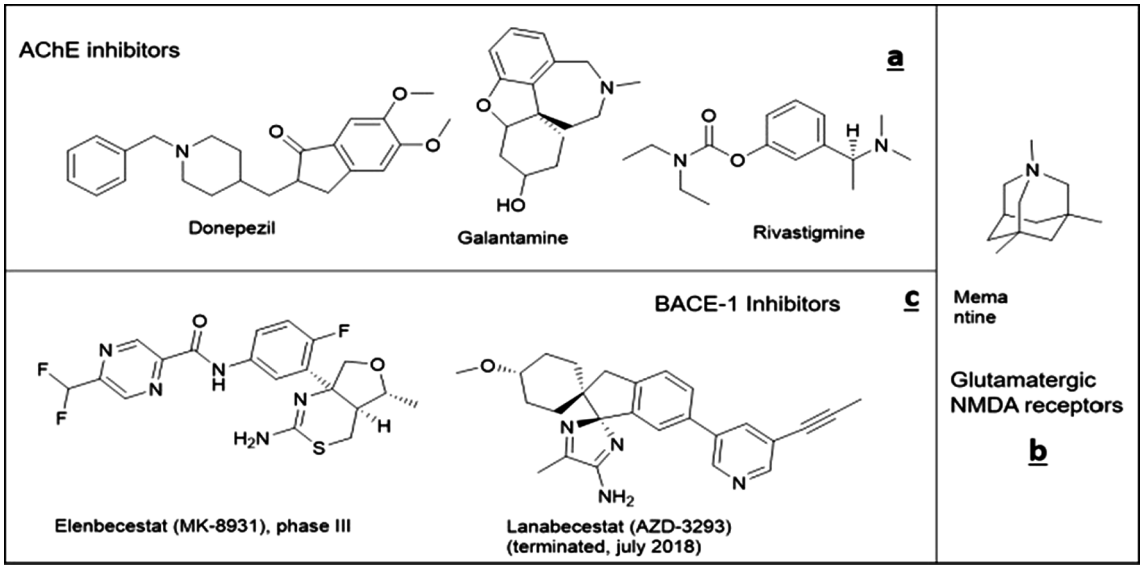

Fig. 1. Structures of FDA-approved treatments for Alzheimer's (a – b) and derivatives BACE-1 inhibitors ongoing and recently discontinued(c).

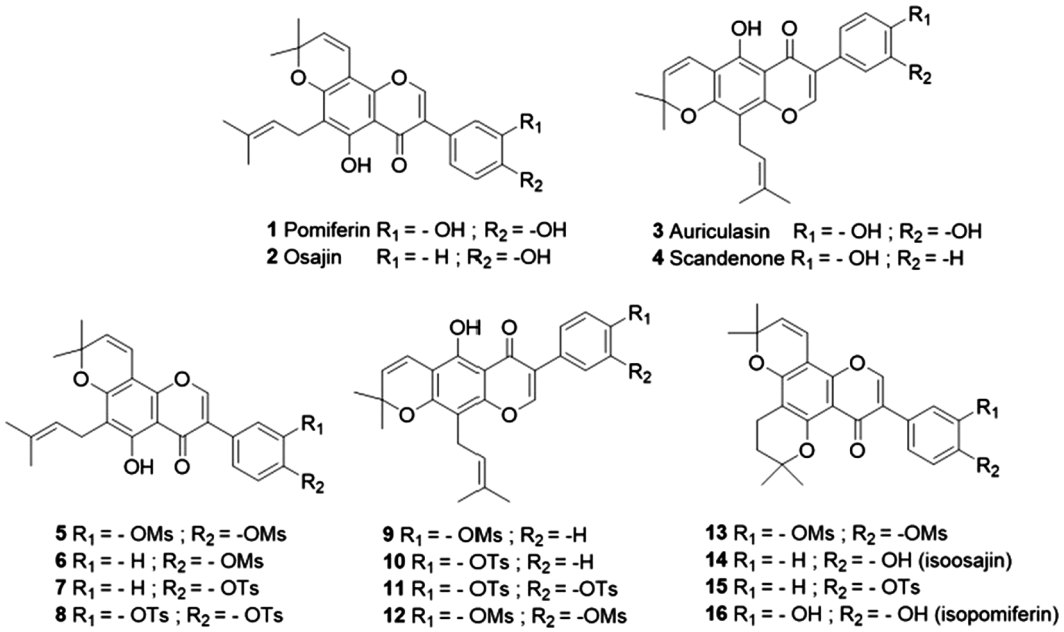

Fig. 2. Structures of natural compounds **1**–**4** and derivatives synthesized and investigated **5** – **16**.

alternative "lead compounds" to be developed as novel therapeutic remedy against CNS-related diseases [6]. For example, flavonoids are well known natural compounds possessing a broad range of pharmacological neuroprotective properties related to AD [7a], such as supressive effect on AChE activities [7b], Aβ fibril formation [7c], and H_2O_2 – induced ROS formation [7d]. Recent studies have demonstrated that isoflavonoids such as genistein and biochanin A, are able to inhibit the activity of BACE-1 [8].

We have previously described the biochemical properties of derivatives derived from Pomiferin **1** and Osajin **2**, which have been confirmed as a phosphodiesterase inhibitors [9]. These two isoflavones isolated from *Maclura Pomifera* (Osage orange) were also found to exhibit anti-cancer [10a], anti-bacterial [10b] and anti-diabetic properties [10c]. In this study, we further investigated the potential application of using semi-synthetic isoflavones as BACE-1 inhibitors and P-gp modulators for modulating AD. We performed accurate and wide *in silico* studies on this class of molecules focusing on the computational definition of their physical and chemical properties, and their possible mode of interaction with the target enzyme BACE-1 and P-gp. These preliminary results were validated by *in vitro* test performed for the evaluation of the efficacy of these compounds. By using cytotoxicity assay, we further confirmed that these compounds are not toxic towards both normal and cancerous cells. Most importantly, among all derivatives which showed promising inhibitory activity towards BACE-1 with the activation on the activity of P-gp, compound **7** is the most promising candidate.

2. Result and discussion

2.1. Chemistry

Auriculasin (**3**) and Scandenone (**4**) are defined as 'chemically constitutional isomers' of pomiferin (**1**) and osajin (**2**), and are the well-known isoflavones that can be isolated from *M. pomifera* fruits [11]. In

fact, these fruits are rich sources of both sets of isomers, which can be extracted with a Soxhlet apparatus. Ethyl acetate or diethyl ether were used as the extraction solvent, followed by an opportune separation procedure to obtain **1** and **2**, while chloroform was used to isolate **3** and **4**. Despite the very close structural similarity among these molecules, 'diagnostic peaks' in the ^{1}H NMR spectrum and NOESY NMR experiment allow to unambiguously distinguish the compounds and to identify the correct structures [9,11].

We performed the extraction of **1 – 4** according to a previously described procedure that allows the acquisition of the two couples of isomers in comparable yields [12].The natural and semi-synthetic derivatives (Fig. 2) that were prepared starting from these four isoflavones were fully characterized by ^{1}H and ^{13}C NMR and high-resolution mass spectrometry. The purity profile was assessed by HPLC.

Isoosajin (**14**) and isopomiferin (**16**) were synthesized by adapting the procedure reported by Wolfrom et al. which heat the natural compounds in acetic and sulfuric acid [13]. These compounds were synthesized with the aim of exploring the effect of an increased rigidity of the scaffold, together with a reduced flexibility and mobility of the side chains. Nevertheless, such modifications on osajin and pomiferin structures led to the loss of one hydrogen bond donor site on the molecules. The synthesized compounds were also used as intermediates for the preparation of the derivatives described below.

The preparation of methanesulfonate and 4-methylbenzenesulfonate derivatives was carried out according to a procedure previously described by Wolfrom et al. [13] However, these authors only proposed the preparation of the 4-methylbenzenesulfonate derivatives of pomiferin and osajin and their cyclized isoosajin and isopomiferin analogues. We therefore synthesized these molecules by reacting other structurally related isoflavones under similar experimental conditions (Supporting information, Scheme 1 and 2). Moreover, we expanded the chemical class by introducing the methanesulfonate moiety (Supporting information, Scheme 1–4). The introduction of the -SO_2R moiety was carried out to explore the effects of extending the bulkiness of the molecule in the phenyl region, and to shade the hydroxyl groups, and thereby introduced a novel hydrogen bond acceptor [14]. This modification is particularly useful because these new functional groups interact strongly with the positive charged amino-acids in the region immediately closed to the active site of BACE-1 as revealed by docking studies. The preparation of such compounds were carried out by reacting the opportune osajin or pomiferin derivative with methanesulfonyl chloride or 4-methylbenzenesulfonyl chloride in pyridine, according to the procedure described in the experimental section. The newly synthesized compounds are shown in Fig. 2.

2.2. In vitro BACE-1 inhibitory activity assay

With the recognition of BACE-1 proteases as a key player in the cleavage of amyloid precursor protein (APP) to produce toxic Aβ peptide, the development of BACE-1 inhibitors has become one of the most promising approaches in AD drug discovery. By adopting a fluorometric-based method utilizing a secretase-specific peptide conjugated to the reporter molecules (EDANS and DABCYL), uncleaved peptide showed the basal fluorescent emissions from EDANS, due to the quenching by the physical interaction of the DABCYL. In contrast, cleavage of the peptide by β- secretase leads to the physical separation of EDANS and DABCYL, resulting in the emission of fluorescent signal (Ex/ Em = 345/500 nm), which is proportional to the β-secretase enzymatic activity. As shown in Fig. 3, compounds **7**, **8, 9, 10** and **13** with their IC_{50} value in BEAS-2B normal cells showed the most potent inhibitory effect on β-secretase enzymatic activity, suggesting their potential inhibitory effect on Aβ peptide level.

2.3. Cytotoxic effect in human cancerous and normal cells

To support the above reported predictions, cell viability assay was performed to study the cytotoxic effect of these compounds in different cells lines.

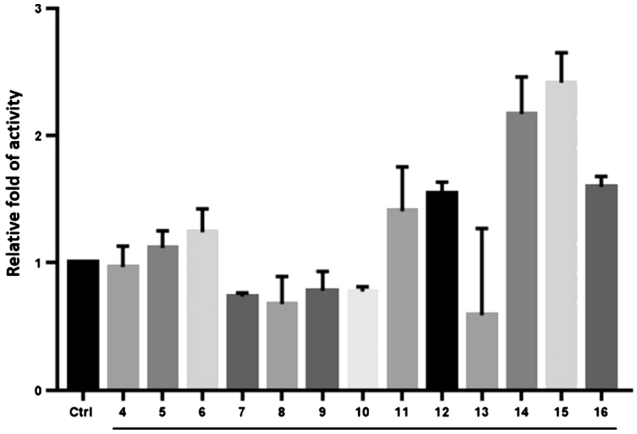

Fig. 3. β-secretase activity of compounds **4–16.**

The cytotoxicity of the analysed compounds was examined in normal human hepatocytes, LO2 and normal lung epithelial cells, BEAS-2B. Among the 16 investigated compounds, 62% and 56% of the compounds showed no cytotoxicity in both normal liver LO2 and lung BEAS-2B cell lines (Table 1, Supporting information Table 2 and 3). Moreover, compounds were also examined on human liver and lung cancer cell lines (HepG2 and A549 (Table 1, Supporting information Table 5 and 6). Results confirmed that compounds **7**, **8** and **13** showed no cytotoxicity on both cancer cells lines while compounds **1** and **2** and respective isomers **14** and **16** revealed moderate cytotoxicity (IC_{50} 13–32 μM) on HepG2 cell lines. Compound **9** present better selectivity for lung cancer A549 cell lines (5 times).

Derivatives **7**, **8, 10** and **13** with potent inhibitory effect on β-secretase enzymatic activity showed no toxicity in all tested cell lines. Natural compounds **1** and **2** and respective isomers **14** and **16** were also evaluated for their cytotoxicity against normal human lung fibroblasts CCD19Lu showed moderate cytotoxicity (IC_{50} 22–64 μM). (Supporting information Table 4).

2.4. Activity of isoflavones derivatives *4 – 16* on P-gp

The pathogenesis of AD may be caused by an imbalance between β-

Table 1
Cytotoxicity of **1–16** against against human liver HepG2, lung A549 cancer cell lines, the normal human hepatocytes, LO2 and normal lung epithelial cells, BEAS-2B.

Compounds	BEAS-2B cells IC_{50} [μM]	A549 cells IC_{50} [μM]	LO2 cells IC_{50} [μM]	HEPG2 cells IC_{50} [μM]
Donezepil[a]	n/a	> 200	n/a	n/a
1	9.8	50.09	15.8	18.9
2	16.9	48.6	70.01	31.4
3	13.4	n/a	n/a	n/a
4	18.9	36.3	22.8	41.2
5	> 100	> 100	> 100	> 100
6	> 100	> 100	86.1	> 100
7	> 100	> 100	> 100	> 100
8	> 100	> 100	> 100	> 100
9	92.6	18.4	42.6	88.1
10	> 100	> 100	> 100	> 100
11	> 100	> 100	> 100	> 100
12	> 100	> 100	> 100	> 100
13	> 100	> 100	> 100	> 100
14	18.2	21.2	11.3	13.1
15	> 100	> 100	> 100	> 100
16	14.1	> 100	11.8	28

[a] Ref. [27].

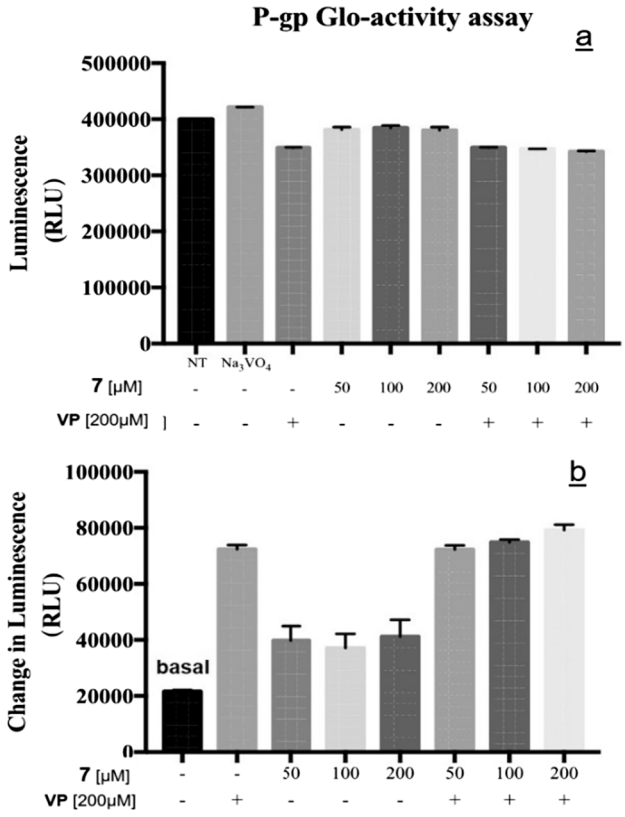

Fig. 4. Stimulation of P-gp ATPase activity by Verapamil (VP) and **7**. Verapamil, which is supplied as a positive control substrate with the Pgp-Glo™ Assay System. Untreated (NT), 100 μM Na_3VO_4- and 200 μM Verapamil-treated Pgp reactions were performed according to the protocol described in experimental section. Luminescence was read on a SpectraMax Paradigm Multi-Mode Microplate Reader (Panel a). The decrease in luminescence of NT samples compared to samples plus Na_3VO_4 (ΔRLUbasal) represents basal Pgp ATPase activity. The decrease in luminescence of Verapamil-treated samples (ΔRLUTC, TC test compound) represents Verapamil-stimulated Pgp ATPase activity. ΔRLUbasal and ΔRLUTC were replotted (Panel b) to illustrate the stimulation of Pgp ATPase activity by Verapamil and **7** (see Supp. inform. Table 9B).

amyloid peptide (Aβ) production and clearance. Some studies reported that β-amyloid is also a substrate for P-gp, and *in vitro* blocking of P-gp functions decreases its clearance across the BBB [5]. For instance, rivastigmine enhanced clearance of Aβ through up-regulation of P-gp [15]. Therefore, targeting β-amyloid clearance by P-gp stimulation could be a useful strategy to prevent AD progression [16]. The biological evaluation of compounds **7**, **8** and **13** was carried out in A549 tumor cell lines [16]. In this assay, rhodamine-123, a fluorescent probe, is used as the P-gp or MRP1 substrate. Recently [17] we have demonstrated that isoflavones pomiferin and isopomiferin are strong P-gp inhibitors (10 μM) in comparison with **VP** in multidrug resistant cancer cells (Supporting information, Table 7). At low concentration (100 μM), we found slightly inhibitory effects of **8** and **13** on P-gp of A549 cancer cells, while compound **7** showed significant decreasing of rhodamine different towards control (Supporting information, Table 8).

We then further evaluated the effects of compound **7** on P-gp ATPase activity. Drug stimulated P-gp ATPase activity was estimated by P-gp-Glo assay system (Promega, Madison, WI) and the results were shown in Fig. 4 and Supporting information Table 9. This method relies on the ATP dependence light-generating reaction of firefly luciferase where ATP consumption is detected as a decrease in luminescence (Fig. 4a). The greater extent on the drop of luminescence signal indicates the stronger the P-gp activity. Here, sodium orthovanadate Na_3VO_4 was used as a P-gp ATPase inhibitor, whereas verapamil (200 μM, VP) was used as a P-gp stimulator. While compounds **7** (tested

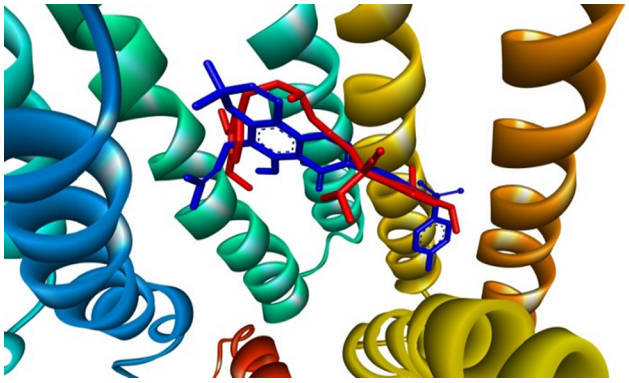

Fig. 5. Docking pose of Verapamil (red) and compound **7** (blue) in binding site of P-gp. (For interpretation of the references to colour in this figure legend, the reader is referred to the web version of this article.)

at 50 μM, 100 μM and same concentration of **VP**) with luminescence signal lower than the control (NT) is considered as a P-gp stimulator, compounds with luminescence signal higher than the NT are considered as P-gp inhibitors. Compounds which are not significantly different from the NT are neither P-gp stimulator nor inhibitor (Supporting information Table 9). Compound **7** was demonstrated as a novel P-gp stimulator (Fig. 4b, at 100 μM, Supporting information Table 8 and 9) that might influence efflux of β amyloid across the BBB.

With the presence of both compounds **7** and **VP,** no further enhancement of P-gp ATPase activity confirmed the docking results which suggested both compound **7** and **VP** are binding and competing for same binding domain of P-glycoprotein (Fig. 5). Moreover, [18] derivative indolizin sulfone SR3357, containing benzenesulfonyl core similarly to **7**, was found interacting with a multiple binding sites on P-gp which are allosterically linked and have differential effect on the ATPase activity of the protein. Therefore, further research work to evaluate the stimulating effects of **7** on efflux of Aβ by P-gp is required [16,19] in coming future.

2.5. Molecular docking studies and in silico physicochemical prediction

In computational study, we first focused on the pharmacokinetic properties of the new compounds, and in particular on those parameters, for example, logP, Topological polar surface area (TPSA) and lipophilicity in general, that are fundamental for crossing the Blood Brain Barrier (BBB). The "drug likeness" of this selected set of compounds was therefore investigated and predicted for their pharmacokinetic properties by using *Molinspiration Cheminformatics software* (http://www.molinspiration.com). We considered the logP value, which is also known to reflect the key physical properties of compounds such as solubility, lipophilicity and bioavailability. TPSA, volume and molecular weight, which are respectively expressed in Å2, Å3 and Da, provide information on the bulkiness of the molecule and the properties of its surface. The number of hydrogen bond donors (nONH) and hydrogen bond acceptors (nON) described the specificity of the recognition between ligand and substrate, and helped to define the propensity of the molecule to generate a-specific interactions with other substrates. The number of rotatable bonds defined the flexibility of the compound. These parameters influence membrane diffusion, transport properties such as blood-barrier crossing and, in general, bioavailability and the percentage of absorption. As reported by Pajouhesh [20], a successful CNS drug or new chemical entity should fulfill certain parameters, such as: MW < 450 Da, clogP < 5, nON < 7, nONH < 3, number of rotatable bonds < 8. The analysis of the pharmacokinetic properties on our synthesized compounds highlighted that while some of them only partially met the above requirements, the most promising candidates satisfied with these conditions more closely (Supporting information Table 1).

These data help to identify the compounds with good oral bioavailability and penetration rate to the central nervous system (CNS), and provide the crucial parameter needed for the design of BACE-1 inhibitors.

However, it was observed that all extracted natural compounds (**1** – **4**), demonstrated negative score and hence were not considered as a BBB penetrant. All compounds containing sulfonic portions showed value above the threshold of 0.02, demonstrating the introduction of $–SO_2R$ moiety may help to increase the penetration rate of compound to BBB. Previous studies reported the addition of sulphates for dopamine [21a] and steroids [21b,21c] could increase their BBB permeation as sulphate group is known substrate of specific transporters. While the active compounds **7**, **8**, **9**, **10** and **13** (Supporting information table 1) possessed scores ranging from 0.055 in compound **9** to a a maximum value of 0.105 in compound **13**, compounds **11** and **15** showed a significant high score in BBB permeation as revealed by in silico study, although with no inhibitory activity on BACE-1 observed *in vitro* (Fig. 3).

Accordingly, an accurate docking study has been performed to understand the mode of interaction of our compounds with BACE-1 and P-gp.

Following a blind docking technique, the preliminary virtual screening has shown that all tested compounds were able to interact selectively and strongly with the active site of BACE-1, as showed in Fig. 6B. Based on the results of this preliminary *in silico* study, compounds **7**, **8**, **11**, **14** and **15** appeared to be the most promising candidates. Comparing these results with the *in vitro* activities, a direct correlation rises with compounds **7** and **8** being identified as the most potent inhibitors of BACE-1.

Together with all the compounds which showed activities in *in vitro* tests, compounds **9**, **10** and **13** were further investigated by using further in silico study with higher accuracy, and with the focus limiting into the active site of the enzyme and the surrounding area (Supporting information Fig. 2). Interestingly, this experiment has demonstrated a defined pattern of interaction between those biologically active compounds. As reported in the 2D interactions plots in Fig. 7 and in the Supporting information Fig. 2a-e, the active compounds formed several H-bonds, especially with the Arg235 and Asn233 residues, exploiting their sulfonic portions.

These interactions were maintained by almost all the active compounds. Other hydrophobic interactions occurred between BACE-1 and the active compounds, such as the interactions with Phe108, Trp115, Ile118 and Leu30 residues.

The common pattern of interaction, together with the binding energies of the active compounds, are correlated with their biological properties. Indeed, the energies of interaction, expressed in Kcal/mol, fit very well with the decrease of activity of the enzyme. This result further confirmed the relevance of this set of compounds as inhibitors of BACE-1. Moreover, considering the obtained energy values for the tested compounds, they were comparable or even better than the calculated energy for the oxazine-based compound [22a] which has been co-crystalized with BACE-1 (PDB ID: 5CLM) (Supporting information Fig. 1a). Nevertheless, it must be pointed out that the predicted interactions of the isoflavones seem to exclude a direct enrollment of the catalytic dyad formed by Asp 32 and Asp 228. Thus, further modification of the proposed scaffold with the aim of directly interfering with these amino acids could represent an interesting improvement in term of drug specificity and potency.

A second set of in silico experiments have been conducted to evaluate and identify the possible site of interaction within P-gp and the allosteric modulators [22b]. Also, blind docking has been adopted to evaluate the most promising compounds (**7**, **8**, **13**). Verapamil (**VP**) was used as a positive control drug for validating the possible site of action of the tested compounds. All these compounds, excluding derivative **13**, interacted with the same pocket within the P-gp with their energies of interactions correlated positively with the obtained biological results (Supporting information Fig 1b). As reported in the 2D interactions plots in the Supporting information Fig. 3a-e, the active compounds presented different modes of interaction with P-gp. As shown in Fig. 5, the pose of **VP** within P-gp strongly overlapped to that of compound **7**, which is the most promising candidate from all of the tested compounds. Compound **7** exhibits two hydrogen bonds with the Tyr303 and the Gly222 exploiting their sulfonic portion, generating the important π-π stacking with the amino acids Tyr306 and Phe299, which positions were also involved in binding pose of verapamil. Several other hydrophobic interactions contributed to the binding energy of our leader compound (Supporting information Fig 1b).

3. Conclusion

The prenylated isoflavones obtained from the derivatization of natural flavonoids from *Maclura pomifera* showed promising *in vitro* and *in silico* results in terms of BACE-1 inhibition and P-gp stimulation. The compounds were evaluated for their oral bioavailability, blood brain barrier permeability and drug likeliness in general (folding, polarity, and molecular size).

The present study demonstrated that prenylated isoflavones in particular **7**, **8** and **13** are active on BACE-1. Furthermore, our result provided important mechanistic insights into the binding mechanism to the enzyme. Moreover compound **7** showed stimulating effect on efflux

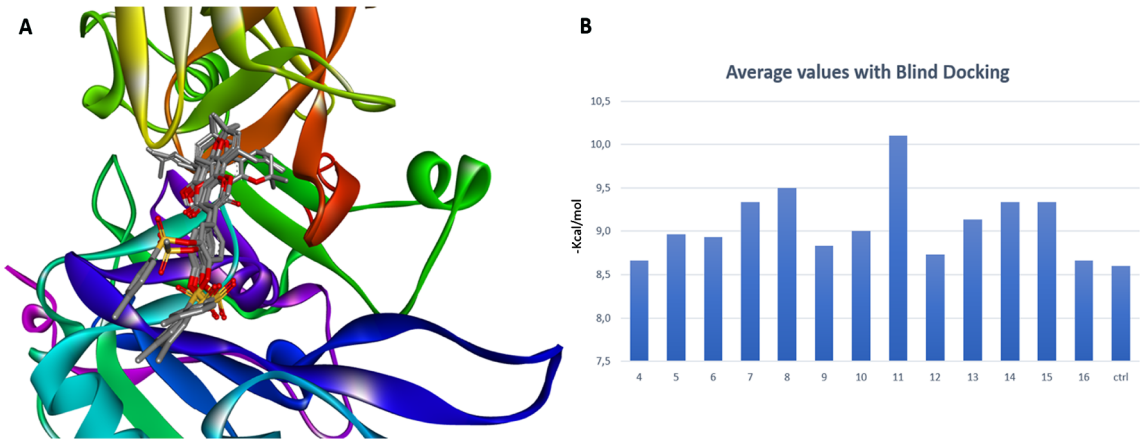

Fig. 6. A. Superimposition of all the best poses of the active molecules that confirm the hypothesis of a common site of action (for the singular poses of the most promising compounds see the Supporting information). **B.** Average values, of three different experiments, of the energies of interactions between BACE-1 and each tested compound.

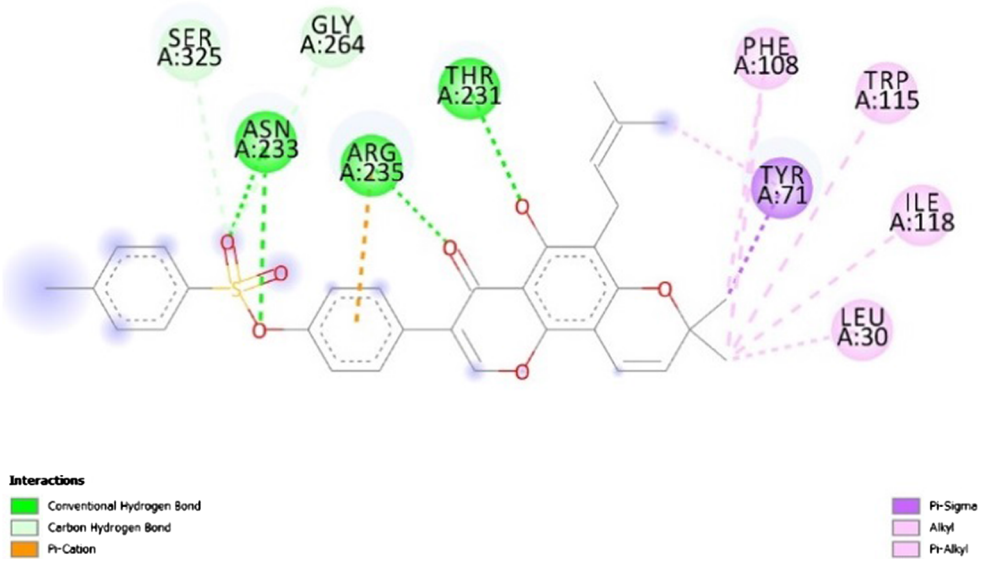

Fig. 7. 2D interaction plot of the compound **7** within the active site of BACE-1.

of rhodamine and P-gp ATPase activity. The current study provided for the first time the important preliminary information for identifying and characterizing prenylated isoflavones as dual targets for the treatment and/or prevention of AD.

4. Experimental

4.1. General

Human normal hepatocytes, LO_2, lung epithelial cells, BEAS-2B and human normal fibroblasts, CCD19Lu were all purchased from ATCC. Cells were cultured in RPMI-1640 medium supplemented with 10% fetal bovine serum and antibiotics penicillin (50 U/ml) and streptomycin (50 μg/ml; Invitrogen, U.K.). All cells were incubated at 37 °C in a 5% humidified CO_2 incubator).

4.2. Chemistry

Commercially available chemicals were purchased from Aldrich unless otherwise stated. ^{1}H and ^{13}C {^{1}H} NMR spectra were recorded on a Bruker Avance III 400 MHz spectrometer and on a Bruker AMX 300 MHz spectrometer. All spectra were recorded at room temperature, the solvent for each spectrum is given in parentheses. Chemical shifts are reported in ppm and are relative to TMS internally referenced to the residual solvent peak. Datasets were edited with Bruker TopSpin suite and iNMR. The multiplicity of signals is reported as singlet(s), doublet (d), triplet (t), quartet (q), multiplet (m), broad (br) or a combination of any of these. High resolution mass spectra (HRMS) were recorded on a ESI–TOF Mariner from Applied Biosystems using electrospray ionization (ESI). The purity profile of the compounds was assayed by HPLC using a Varian Pro-Star system equipped with a Biorad 1706 UV–VIS detector and an Agilent C-18 column (5 μm, 4.6 × 150 mm). An appropriate ratio of water (A) and acetonitrile (B) was used as mobile phase with an overall flow rate of 1 mL min^{-1}. The general method for the analyses is reported here: 0 min (90% A–10% B), 5 min (90% A–10% B), 25 min (10% A–90% B), 30 min (90% A–10% B), and 32 min (90% A–10% B). The purity of all compounds was ≥96%, unless otherwise stated (254 nm).

4.3. General procedure for isolation of pomiferin (1) and osajin (2), auriculasin (3) and scandenone (4)

Compounds were extracted with a Soxhlet apparatus from. Ethyl acetate or diethyl ether were used as the extraction solvent, followed by an opportune separation procedure to obtain **1** and **2**, while chloroform was used to isolate **3** and **4**.

4.3.1. Characterization of 7-(3,4-dihydroxyphenyl)-9-hydroxy-2,2-dimethyl-10-(3-methyl-2-butenyl)-1,5-dioxa-2H-phenanthren-8-one (1, pomiferin)

Yield: 0.7 g from 200 g of dried *M. pomifera* fruits. δH (400 MHz, $CDCl_3$): 12.97 (1H, s, OH), 7.89 (1H, s, C═CH), 7.04 (1H, d, *J* 1.1 Hz, Ar-H), 6.84 (1H, d, *J* 7.1 Hz, C═CH), 6.71 (1H, dd, *J* 7.1 Hz, Ar-H), 5.56 (1H, d, *J* 10 Hz, C═CH), 5.24 (1H, m, C═CH), 3.36 (2H, d, *J* 7.0 Hz, CH_2), 1.82 (3H, s, CH_3), 1.69 (3H, s, CH_3), 1.50 (6H, s, CH_3). δC (100 MHz, $CDCl_3$): 181.2, 159.3, 157.4, 152.6, 150.4, 144.8, 144.1, 131.6, 127.4, 123.8, 122.8, 121.9, 121.8, 116.6, 115.6, 115.2, 113.2, 105.6, 100.9, 77.8, 28.3, 26.2, 21.6, 18.1. HMRS (ESI) found 421.1653, calc. 421.1646 Anal. found C 71.5, H 5.8. Calc. for $C_{25}H_{24}O_5$: C 71.4, H 5.8.

4.3.2. Characterization of 9-hydroxy-7-(p-hydroxyphenyl)-2,2-dimethyl-10-(3-methyl-2-butenyl)-1,5-dioxa-2H-phenanthren-8-one (2, osajin)

Yield: 4.0 g from 200 g of dried *M. pomifera* fruits. δH (400 MHz, $CDCl_3$): 13.14 (1H, s, OH), 7.88 (1H, s, C═CH), 7.39 (2H, m, Ar-H), 6.89 (2H, m, *J* 8.1 Hz, ArH), 6.70 (1H, d, *J* 10 Hz, C═CH), 5.59 (1H, d, *J* 10 Hz, C═CH), 5.26 (1H, m, *J* 7.3 Hz, C═CH), 5 (1H, s, OH), 3.37 (2H, d, *J* 7.3 Hz, CH_2), 1.83 (3H, s, CH_3), 1.70 (3H, s, CH_3), 1.50 (6H, s, CH_3). δC (100 MHz, $CDCl_3$): 181.1, 159.3, 157.4, 155.0, 152.4, 150.6, 131.7, 130.5, 127.3, 123.7, 123.0, 122.0, 115.8, 115.1, 113.0, 105.6, 100.8, 77.9, 28.3, 26.0, 21.4, 18.0. HMRS (ESI) found 405.1669, calc. 406.1697 Anal. found C 74.1, H 6. Calc. for $C_{25}H_{24}O_5$: C 74.2, H 6.

4.3.3. Characterization of 7-(3,4-dihydroxyphenyl)-5-hydroxy-2,2-dimethyl-10-(3-methylbut-2-enyl)pyrano[3,2–g]chromen-6-one (3, auriculasin)

Yield: 0.8 g from 200 g of dried *M. pomifera* fruits. δH (400 MHz, $CDCl_3$): 13.46 (1H, s, OH), 7.80 (1H, s, C═CH), 6.94 (1H, d, *J* 1.1 Hz, Ar-H), 6.73 (1H, d, *J* 7.1 Hz, C═CH), 6.89 (1H, dd, *J* 7.1 Hz, Ar-H), 6.65 (1H, dd, *J* 10.0 Hz, C═CH), 5.67 (1H, d, *J* 10 Hz, C═CH), 5.20 (1H, m, C═CH), 5.03 (1H, s, OH), 3.32 (2H, d, *J* 7.0 Hz, CH_2), 1.80 (3H, s, CH_3), 1.65 (3H, s, CH_3), 1.48 (6H, s, CH_3). δC (100 MHz, $CDCl_3$): 182.0, 156.2, 156.0, 154.9, 150.1, 144.6, 144.1, 131.6, 127.1, 123.8, 122.2, 121.9, 121.0, 116.6, 115.9, 115.6, 113.2, 108.4, 100.9, 77.8, 28.3, 26.7, 22.1, 17.2. HMRS (ESI) found 421.1652, calc. 421.1646 Anal. found C 71.5, H 5.8. Calc. for $C_{25}H_{24}O_5$: C 71.4, H 5.8.

*4.3.4. Characterization of 5-hydroxy-7-(4-hydroxyphenyl)-2,2-dimethyl-10-(3-methylbut-2-enyl)pyrano[3,2–g]chromen-6-one (**4**, Scandenone)*

Yield: 3.6 g from 200 g of dried M. pomifera fruits. δH (400 MHz, $CDCl_3$): 7.89 (1H, s, C═CH), 7.35 (2H, m, Ar-H), 6.84 (2H, m, *J* 8.1 Hz, ArH), 6.74 (1H, d, *J* 10 Hz, C═CH), 5.63 (1H, d, *J* 10 Hz, C═CH), 5.17 (1H, m, *J* 7.3 Hz, C═CH), 5 (1H, s, OH), 3.40 (2H, d, *J* 7.3 Hz, CH_2), 1.81 (3H, s, CH_3), 1.68 (3H, s, CH_3), 1.47 (6H, s, CH_3). δC (100 MHz, $CDCl_3$): 181.4, 159.2, 157.4, 155.9, 152.6, 150.6, 131.2, 130.5, 127.1, 123.7, 123.0, 121.9, 115.8, 115.6, 113.0, 105.6, 100.8, 77.9, 28.3, 25.7, 21.3, 17.9. HMRS (ESI) found 405.1670, calc. 405.1697 Anal. found C 74.1, H 6. Calc. for $C_{25}H_{24}O_5$: C 74.2, H 6.

4.4. General procedure for the preparation of methanesulfonate derivatives

A round bottom flask was charged with the opportune isoflavone (200 mg) and 2 mL of pyridine. A solution of 0.6 mL of methanesulfonyl chloride in pyridine (3 mL) was added and the resulting mixture was stirred at room temperature. The reaction was monitored by TLC (hexane/ethyl acetate 1:1) and, after completion, it was quenched by pouring the mixture in cold water. The resulting solid was collected by filtration and recrystallized from ethanol.

*4.4.1. Characterization of 4-(5-hydroxy-8,8-dimethyl-6-(3-methylbut-2-en-1-yl)-4-oxo-4,8-dihydropyrano[2,3–f]chromen-3-yl)-1,2-phenylene dimethanesulfonate (**5**)*

Yield: 71%. δH (400 MHz, $CDCl_3$): 12.88 (1H, s, OH), 7.98 (1H, s, C═CH), 7.74 (1H, m, Ar-H), 7.57 (2H, m, Ar-H), 6.70 (1H, d, *J* 9.9 Hz, C═CH), 5.62 (1H, d, *J* 9.9 Hz, C═CH), 5.23 (1H, m, C═CH), 3.36 (2H, d, *J* 7.1 Hz, CH_2), 3.31 (3H, s, CH_3), 3.30 (3H, s, CH_3), 1.83 (3H, s, CH_3), 1.70 (3H, s, CH_3), 1.51 (6H, s, CH_3). δC (100 MHz, $CDCl_3$): 182.1, 161, 159.2, 154.6, 150.9, 133.5, 132.3, 132.2, 129.1,124.3, 124, 123.5, 116.5, 115, 107.2, 102.6, 79.7, 78.4, 39.2, 29.9, 27.5, 23, 19.7. HMRS (ESI) found 577.1642, calc. 577.1124 Anal. found C 56.1, H 4.9, S 11.1. Calc. for $C_{27}H_{28}O_{10}S_2$: C 56.2, H 4.9, S 11.1%.

*4.4.2. Characterization of 4-(5-hydroxy-8,8-dimethyl-6-(3-methylbut-2-en-1-yl)-4-oxo-4,8-dihydropyrano[2,3–f]chromen-3-yl)phenyl methanesulfonate (**6**)*

Yield: 69%. δH (400 MHz, $CDCl_3$): 13.02 (1H, s, OH), 7.93 (1H, s, C═CH), 7.60 (2H, d, *J* 8.8 Hz, Ar-H), 7.38 (2H, d, *J* 8.8 Hz, Ar-H), 6.71 (1H, d, *J* 9.9 Hz, C═CH), 5.61 (1H, d, *J* 9.9 Hz, C═CH), 5.25 (1H, m, C═CH), 3.36 (2H, d, *J* 7.1 Hz, CH_2), 3.20 (3H, s, CH_3), 1.83 (3H, s, CH_3), 1.71 (3H, s, CH_3), 1.50 (6H, s, CH_3). δC (100 MHz, $CDCl_3$): 180.3, 159.2, 157.4, 152.8, 150.4, 149.1, 131.7, 130.6, 130.4, 127.4, 122.5, 122.1, 121.7, 114.7, 113.1, 105.4, 100.8, 78, 37.4, 28.1, 25.8, 21.3, 17.9. HMRS (ESI) found 483.1695, calc. 483.1399. Anal. found C 64.7, H 5.4, S 6.5. Calc. for $C_{26}H_{26}O_7S$ C 64.7, H 5.4, S 6.6%.

*4.4.3. Characterization of 4-(5-hydroxy-8,8-dimethyl-10-(3-methylbut-2-en-1-yl)-4-oxo-4,8-dihydropyrano[3,2–g]chromen-3-yl)phenyl methanesulfonate (**9**)*

Yield: 55%. δH (400 MHz, $CDCl_3$): 13.00 (1H, s, OH), 7.93 (1H, s, C═CH), 7.59 (2H, d, *J* 8.8 Hz, Ar-H), 7.40 (2H, d, *J* 8.8 Hz, Ar-H), 6.70 (1H, d, *J* 9.9 Hz, C═CH), 5.61 (1H, d, *J* 9.9 Hz, C═CH), 5.25 (1H, m, C═CH), 3.38 (2H, m, CH_2), 3.20 (3H, s, CH_3), 1.83 (3H, s, CH_3), 1.70 (3H, s, CH_3), 1.50 (6H, s, CH_3). δC (100 MHz, $CDCl_3$): 180.2, 156.7, 155.5, 154.2, 154.0, 153.1, 131.8, 131.2, 129.1, 124.1, 122.2, 120.9, 116.1, 108.1, 103.1, 78.2, 37.1, 29.1, 28.1, 25.9, 21.3, 18.0. HMRS (ESI) found 483.1695, calc. 483.1399. Anal. found C 64.8, H 5.4, S, 6.5. Calc. for $C_{26}H_{26}O_7S$: C 64.7, H 5.4, S, 6.6%.

*4.4.4. Characterization of 4-(5-hydroxy-8,8-dimethyl-10-(3-methylbut-2-en-1-yl)-4-oxo-4,8-dihydropyrano[3,2–g]chromen-3-yl)-1,2-phenylene dimethanesulfonate (**12**)*

Yield: 67%. δH (400 MHz, $CDCl_3$): 12.77 (1H, s, OH), 7.98 (1H, s, C═CH), 7.74 (1H, m, Ar-H), 7.58 (2H, m, Ar-H), 6.72 (1H, d, *J* 9.9 Hz, C═CH), 5.64 (1H, d, *J* 9.9 Hz, C═CH), 5.26 (1H, m, C═CH), 3.37(2H, d, *J* 7.1 Hz, CH_2), 3.31 (3H, s, CH_3), 3.30 (3H, s, CH_3), 1.83 (3H, s, CH_3), 1.70 (3H, s, CH_3), 1.51 (6H, s, CH_3). δC (100 MHz, $CDCl_3$): 180.3, 156.4, 154.6, 151.0, 132.2, 130.4, 130.2, 127.3, 122.2, 121.5, 119.3, 116.2, 115.4, 112.6, 110.2, 109.8, 108.9, 108.2, 107.2, 105.4, 102.1, 77.1, 29.1, 28.5, 25.2, 21.6, 17.9. HMRS (ESI) found 577.1642, calc. 577.1124. Anal. found C 56.2, H 4.9, S 11.1. Calc. for $C_{27}H_{28}O_{10}S_2$: C 56.2, H 4.9, S 11.1%.

*4.4.5. Characterization of 4-(2,2,10,10-tetramethyl-8-oxo-8,10,11,12-tetrahydro-2H-dipyrano[2,3-f:2′,3′-h]chromen-7-yl)-1,2-phenylene dimethanesulfonate (**13**)*

Yield: 71%. δH (400 MHz, $CDCl_3$): 7.84 (1H, s, C═CH), 7.73 (1H, d, J 1.8, Ar-H), 7.59 (1H, d, *J* 8.4 Hz, Ar-H), 7.53 (1H, d, *J* 8.4 Hz, Ar-H), 6.75 (1H, d, *J* 10.0 Hz, C═CH), 5.60 (1H, d, *J* 10.0 Hz, C═CH), 3.28 (3H, s, CH3), 3.27 (3H, s, CH_3),2.69 (2H, m, CH_2), 1.86 (2H, m, CH_2), 1.52 (6H, s, CH_3), 1.45 (6H, s, CH_3). δC (100 MHz, $CDCl_3$): 182.1, 159.2, 156.1, 152.0, 150.2, 144.5, 140.2, 137.5, 128.1, 119.0, 113.1, 110.0, 108.1, 108.0, 103.1, 102.2, 89.1, 83.5, 38.1, 37.6, 33.3, 29.4, 27.1, 26.1. HMRS (ESI) found 729.1745, calc. 729.1758. Anal. found C 63.1, H 5.1, S 8.8. Calc. for $C_{39}H_{39}O_{10}S_2$: C 63.1, H 5.0, S 8.8%.

4.5. General procedure for the preparation of 4-methylbenzenesulfonate derivatives

A round bottom flask was charged with the opportune isoflavone (100 mg) and 1 mL of pyridine. A solution of 400 mg of 4-methylbenzenesulfonyl chloride in pyridine (2 mL) was added and the resulting mixture was stirred at room temperature. The reaction was monitored by TLC (hexane/ethyl acetate 1:1) and, after completion, it was quenched by pouring the mixture in cold water. The resulting solid was collected by filtration and recrystallized from ethanol.

*4.5.1. Characterization of 4-(5-hydroxy-8,8-dimethyl-6-(3-methylbut-2-en-1-yl)-4-oxo-4,8-dihydropyrano[2,3–f]chromen-3-yl)phenyl 4-methylbenzenesulfonate (**7**)*

Yield 68%. δH (400 MHz, $CDCl_3$): 12.98 (1H, s, OH), 7.89 (1H, s, C═CH), 7.77 (2H, m, Ar-H), 7.49 (2H, m, Ar-H), 7.35 (2H, d, *J* 7.9 Hz, Ar-H), 7.08 (2H, m, Ar-H), 6.69 (1H, d, *J* 9.9 Hz, C═CH), 5.60 (1H, d, *J* 9.9 Hz, C═CH), 5.23 (1H, m, C═CH), 3.36 (2H, m, CH_2), 2.49 (3H, s, CH_3), 1.83 (3H, s, CH_3), 1.70 (3H, s, CH_3), 1.50 (6H, s, CH_3). δC (100 MHz, $CDCl_3$): 180.2, 159.3, 152.8, 145.4, 130.1, 130, 129.8, 128.5, 127.3, 122.4, 121.7, 114.8, 28.1, 25.7, 21.7, 17.9. HMRS (ESI) found 559.2178, calc. 559.1712. Anal. found C 68.9, H 5.4, S 5.6. Calc. for $C_{32}H_{30}O_7S$ C 68.8, H 5.4, S 5.7%.

*4.5.2. Characterization of 4-(5-hydroxy-8,8-dimethyl-6-(3-methylbut-2-en-1-yl)-4-oxo-4,8-dihydropyrano[2,3–f]chromen-3-yl)-1,2-phenylene dimethanesulfonate (**8**)*

Yield: 58%. δH (400 MHz, $CDCl_3$): 12.96 (1H, s, OH), 7.91 (1H, s, C═CH), 7.70 (4H, m, J 1.8, Ar-H), 7.46 (1H, m, Ar-H), 7.46 (1H, m, Ar-H), 7.35 (1H, m, Ar-H), 7.33 (4H, m, Ar-H), 6.69 (1H, d, *J* 9.9 Hz, C═CH), 5.61 (1H, d, *J* 9.9 Hz, C═CH), 5.23 (1H, m, C═CH), 3,36 (2H, d, *J* 7.1 Hz, CH_2), 2.48 (6H, s, CH_3), 1.83 (3H, s, CH_3), 1.70 (3H, s, CH_3), 1.51 (6H, s, CH_3). δC (100 MHz, $CDCl_3$): 180.8, 159.2, 157.5, 145.7, 141, 132.1, 131.7, 129.8, 128.6, 128.5, 125, 124.3, 122.1, 121.7, 28.8, 28.1, 25.9, 21.8. HMRS (ESI) found 729.2207, calc. 729.1750. Anal. found C 64.2, H 5.0, S 8.8. Calc. for $C_{39}H_{36}O_{10}S_2$: C 64.3, H 5.0, S 8.8%.

*4.5.3. Characterization of 4-(5-hydroxy-8,8-dimethyl-10-(3-methylbut-2-en-1-yl)-4-oxo-4,8-dihydropyrano[3,2–g]chromen-3-yl)phenyl 4-methylbenzenesulfonate (**10**)*

Yield: 58%. δH (400 MHz, $CDCl_3$): 13.01 (1H, s, OH), 7.89 (1H, s, C═CH), 7.78 (2H, d, *J* 8.4 Hz, Ar-H), 7.49 (2H, d, *J* 8.7 Hz, Ar-H), 7.36 (2H, d, *J* 8.4 Hz, Ar-H), 7.10 (2H, d, J, 8.7 Hz, Ar-H), 6.71 (1H, d, *J*

9.9 Hz, C═CH), 5.63 (1H, d, *J* 9.9 Hz, C═CH), 5.25 (1H, m, C═CH), 3.38 (2H, m, CH_2), 2.49 (3H, s, CH_3), 1.83 (3H, s, CH_3), 1.69 (3H, s, CH_3), 1.50 (6H, s, CH_3). δC (100 MHz, $CDCl_3$): 178.9, 132.5, 131.6, 130.1, 129.8, 128.5, 127.3, 122.4, 122.5, 77.9, 17.9. HMRS (ESI) found 559.2178, calc. 559.1712. Anal. found C 68.7, H 5.4, S 5.9. Calc. for $C_{32}H_{30}O_7S$: C 68.8, H 5.4, S 5.7%.

*4.5.4. Characterization of 4-(5-hydroxy-8,8-dimethyl-10-(3-methylbut-2-en-1-yl)-4-oxo-4,8-dihydropyrano[3,2–g]chromen-3-yl)-1,2-phenylene bis (4-methylbenzenesulfonate) (**11**)*

Yield: 69%. δH (400 MHz, $CDCl_3$): 12.93 (1H, s, OH), 7.92 (1H, s, C═CH), 7.69 (4H, m, J 1.8, Ar-H), 7.48 (1H, m, Ar-H), 7.46 (1H, m, Ar-H), 7.35 (1H, m, Ar-H), 7.33 (4H, m, Ar-H), 6.69 (1H, d, *J* 9.9 Hz, C═CH), 5.61 (1H, d, *J* 9.9 Hz, C═CH), 5.25 (1H, m, C═CH), 3,36 (2H, m, CH_2), 2.48 (6H, s, CH_3), 1.83 (3H, s, CH_3), 1.70 (3H, s, CH_3), 1.50 (6H, s, CH_3). δC (100 MHz, $CDCl_3$): 159.2, 157.5, 145.7, 141, 132.1, 131.7, 129.8, 128.6, 124.3, 121.7, 77.8, 28.7, 28.1, 25.8, 21.8, 17.9. HMRS (ESI) found 729.2207, calc. 729.1750. Anal. found C 64.2, H 5.1, S 8.8. Calc. for $C_{39}H_{36}O_{10}S_2$: C 64.3, H 5.0, S 8.8.

*4.5.5. Characterization of 4-(2,2,10,10-tetramethyl-8-oxo-8,10,11,12-tetrahydro-2H-dipyrano[2,3-f:2′,3′-h]chromen-7-yl)phenyl 4-methylbenzenesulfonate (**15**)*

Yield: 59%. δH (400 MHz, $CDCl_3$): 7.70 (1H, s, C═CH), 7.53 (2H, d, *J* 8.5 Hz, Ar-H), 7.25 (2H, d, *J* 8.5 Hz, Ar-H), 6.68 (1H, d, J 9.9C═CH), 5.50 (1H, d, *J* 9.9 Hz, C═CH), 3.07 (3H, s, CH_3) 2,61 (2H, m, CH_2), 1.75 (2H, m, CH_2), 1.42 (6H, s, CH_3), 1.45 (6H, s, CH_3). δC (100 MHz, $CDCl_3$): 179.6, 159.8, 153.4, 151.9, 150.1, 143.2, 139.2, 130.1, 128.6, 121.4, 117.4, 113.5, 109.8, 102.7, 101.6, 82.9, 82.0, 40.1, 31.3, 29.1, 28.8, 26.5, 24.9, 19.1. HMRS (ESI) found 559.1717, calc. 559.1720. Anal. found C 68.5, H 5.3, S 5.8. Calc. for $C_{32}H_{30}O_7S$: C 68.4, H 5.2, S 5.8%.

*4.6. Synthesis of Isoosajin (**14**) and isopomiferin (**16**)*

Isoosajin (**14**) and isopomiferin (**16**) were synthesized by adapting the procedure reported by Wolfrom et al. [13]. The reactions were carried out on the opportune intermediates, which were previously isolated from *M. pomifera* fruits according to a previously reported procedure [9]. To perform the cyclization reaction, a round bottom flask was charged with osajin or pomiferin and 7 mL of glacial acetic acid. The mixture was heated to 100 °C and, subsequently, 0.2 mL of sulfuric acid were added dropwise. The mixture was stirred at room temperature and the reaction was monitored by TLC (hexane/ethyl acetate 1:1). The reaction was quenched by pouring the mixture in cold water. The resulting solid was collected by filtration to give the desired product.

*4.6.1. Characterization of 7-(4-hydroxyphenyl)-2,2,10,10-tetramethyl-11,12-dihydro-2H-dipyrano[2,3-f:2′,3′-h]chromen-8(10H)-one (**14**, isoosajin)*

Yield: 75%. δH (400 MHz, $CDCl_3$): 7.77 (1H, s, C═CH), 7.31 (2H, d, *J* 8.5 Hz, Ar-H), 6.88 (2H, d, *J* 8.5 Hz, Ar-H), 6.75 (1H, d, *J* 9.9 Hz, C═CH), 5.56 (1H, d, *J* 9.9 Hz, C═CH), 2.67 (2H, m, CH_2), 1.83 (2H, m, CH_2), 1.50 (6H, s, CH_3), 1.46 (6H, s, CH_3). δC (100 MHz, $CDCl_3$): 158.2, 151.1, 150.8, 150.1, 131.6, 130.0, 129.4, 129.1, 125.2, 115.8, 115.2, 114.8, 114.1, 105.1, 103.1, 79.8, 33.1, 29.8, 25.1, 17.1. HMRS (ESI) found 405.1669, calc. 405.1624. Anal. found C 74.1, H 6.0. Calc. for $C_{25}H_{24}O_5$: C 74.2, H 6.0%.

*4.6.2. Characterization of 7-(3,4-dihydroxyphenyl)-2,2,10,10-tetramethyl-11,12-dihydro-2H-dipyrano[2,3-f:2′,3′-h]chromen-8(10H)-one (**16**, isopomiferin)*

Yield: 65%. δH (400 MHz, $CDCl_3$): 7.83 (1H, s, C═CH), 7.24 (1H, d, *J* 1.9 Hz, Ar-H), 6.88 (1H, d, *J* 8.3 Hz, Ar-H), 6.77 (1H, d, *J* 8.3 Hz, Ar-H), 6.74 (1H, d, *J* 10.0 Hz, C═CH), 5.58 (1H, d, *J* 10.0 Hz, C═CH), 2.69 (2H, m, CH_2), 1.85 (2H, m, CH_2) 1.85 (6H, s, CH_3), 1.47 (6H, s, CH_3). δC (100 MHz, $CDCl_3$): 180.7, 160.1, 157.5, 155.6, 153.1, 150.9, 143.2, 141.2, 141.0, 129.2, 118.7, 110.1, 110.0, 108.6, 106.2, 104.3, 100.3, 87.2, 82.4, 33.2, 28.2, 26.5, 16.3. HMRS (ESI) found 421.1653, calc. 421.1573. Anal. found C 71.4, H 5.8. Calc. for $C_{25}H_{24}O_6$: C 71.4, H 5.8%.

4.7. Biological screening studies

4.7.1. Cytotoxicity drug assay

All test compounds were dissolved in DMSO at a final concentration of 50 mM and stored at −20 °C before use. Cytotoxicity was assessed by using the 3-(4,5-dimethylthiazole-2yl)-2,5-diphenyltetrazolium bromide (MTT) (5 mg/ml) assay as previously described [23]. Briefly, $4x10^3$ cells per well were seeded in 96-well plates before drug treatments. After overnight cell culture, the cells were then exposed to different concentration of selected compounds (0.19–100 μM) for 72 h. Cells without drug treatment were used as control. Subsequently, 10 μl of 5 mg/mL MTT solution was added to each well and incubated at 37 °C for 4 h followed by addition of 100 μl solubilization buffer (10 mM HCl in solution of 10% of SDS) and overnight incubation. A_{570} nm was then determined in each well on the next day. The percentage of cell viability was calculated using the following formula: Cell viability (%) = $A_{treated}/A_{control} \times 100$. A representative graph of at least three independent experiments is shown in Supporting information Table 2–8.

4.7.2. BACE-1 inhibition assay

Assay was performed in a 96-well flat bottom white plate using β-Secretase Activity Fluorometric Assay Kit (Biovision, CA, USA). To begin, 5×10^6 cells were collected by centrifugation with ice-cold extraction buffer added for homogenization. After centrifugation, 50 μl supernatant (cell lysate) was transferred to each well in the 96-well plate. 2 μl of active β-secretase (protein concentration: 4μg/μL) was added to the 50 μl of extraction buffer as the positive control. For negative control, 2 μl of the β-secretase inhibitor was added to the 50 μl sample well. 2 μl of each of the tested samples **4–16** (drug concentration: IC50 value in BEAS-2B cells-Table 1) were added into each sample well for inhibitory activity evaluation. Following compounds addition, 50 μl of 2X reaction buffer was added with gentle mix and incubation for 20 min at 37 °C before adding of 2 μl of β-secretase substrate. The plate was then covered and incubated in the dark at 37 °C for 1 h. Samples were then read in a fluorescent 96-well plate reader (Ex/Em = 345/500 nm). Background readings produced from substrate without the addition of secretase were subtracted from all samples. Secretase activity was calculated as the fold change in secretase activity. A representative graph of at least three independent experiments is shown in Fig. 5.

4.7.3. Rhodamine 123 exclusion assay (P-gp assay)

P-gp activity was determined by measuring intracellular accumulation of rhodamine 123 in A549 cell lines in the absence or presence of P-gp inhibitors. Briefly, cells were incubated at 37C with 10 μM verapamil, 0.5 μM of **1**, 0.5 μM of **3** or 0.5 μM of **6** respectively for 4 h. Subsequently, 5 μg/mL of rhodamine123 was added to each well and the wells were incubated for another 1 h. After washing in phosphate – buffered saline, cells were lysed in distilled water, and intracellular levels of rhodamine 123 were quantified by spectrofluorimetry using CellQuest (BD Biosciences, San Jose, CA, USA). Data were expressed as % of rhodamine 123 accumulation in control cells not exposed to P-gp inhibitors, arbitrarily set at 100%. Experimental data were routinely expressed as means ± SEM from at least three independent experiments using the Prism software (GraphPad software, La Jolla, CA, USA).

4.7.4. P-gp Glo activity assay (ATPase assay)

The activity of P-gp ATPase in response to **7** was determined by Pgp-

Glo assay system (Promega, Madison, WI). According to the manufacture instruction, the stimulatory effect of **7** on the activity of P-gp ATPase was measured. The luminescence of the sample reflects the ATP level in the sample, which is positively correlated with the activity of P-gp ATPase and was recorded using the SpectraMax Paradigm Multi-Mode Microplate Reader (Molecular Devices).

4.8. Molecular properties and drug-likeness of reference compounds

Blood–brain barrier permeation (BBB) was predicted using online BBB permeation predictor software available at http://www.cbligand.org/BBB/. As per the software, any compound having a SVM_MACCSFP BBB score of higher than 0.02 will be considered as able to cross BBB. (Supporting information Table 1)

4.9. Molecular docking studies

All the compounds used for these computational studies have been drawn with ChemDraw and then minimized with Avogadro [24]. For the process of minimization, the appropriate hydrogen atoms were added to all the drawn compounds, considering an environmental pH of 5.5, which is the actual pH at which the enzyme BACE-1 operates. All the structures have been minimized using the MMFF94 forcefield. For what concerns the choice of the enzymatic crystal structure used for the docking assays, several parameters were considered. Firstly, the crystal structures should be complete in the region near the active site and in the surrounding areas. Secondly, we have considered the limitations that this computational method brings with it: the classical docking approach maintains the macromolecular structure of the protein rigid and not able to adapt to the different small molecules that are tested as ligands. For these reasons, several PDB files have been selected, just to avoid bias due by an unusual or unfavorable orientation of the aminoacidic residues within the possible interaction site of our compounds (PDB IDs: 5CLM, 2ZHR, 1M4H), The PDB structures were optimized for the docking studies. All the hydrogens were added considering a pH of 5,5 and then the catalytic dyad composed by Asp32 and Asp228 was controlled and organized in its physiological condition. After the preparation of the PDB files of BACE-1 and of the small molecules, a rough massive screening has been performed with all the synthetized compounds using the software PyRx (https://pyrx.sourceforge.io/). In this first part of the virtual screening, all the three crystal structures of BACE-1 have been used. The whole surface area of the enzyme was used for the docking process (*blind docking*). An average of the energies of interactions (Kcal/mol) obtained with the three different PDB structures have been calculated and reported in Fig. 3b. In the second round, the 5 compounds with the best docking score and all the molecules active in the biological tests have been docked using Autodock Vina [25] reducing the research space within a smaller area around the active site of the enzyme in all the three different crystal structures. As a method validation, we used the oxazine molecule co-crystalized in the 5CLM PDB file observing the pose obtained for this compound and comparing it with that one of the original crystal structure. With all the adopted protocols this molecule assumes the same orientation as in the original crystal structure. The complexes were analyzed using BIOVIA Discovery Studio [26] and the relative 2D interaction plots were obtained. A similar approach has been adopted for performing docking studies of our compounds and P-gp. The molecules were newly minimized at pH 7.2 because the efflux pump work at physiological pH. The chosen crystal structure is the 3G60. We used as a positive control Verapamil. (see the Supporting information for further information about docking studies).

Acknowledgements

This work was supported by a FDCT grant from the Macao Science and Technology Development Fund to VKWW (Project code: 0022/2018/A1) and by University of Padova (GZ).

Conflict of interest

The authors have declared no conflict of interest.

Appendix A. Supplementary material

Supplementary data to this article can be found online at https://doi.org/10.1016/j.bioorg.2019.03.034.

References

[1] (a) M. Wortmann, Alzheimer's Res. Ther. 4 (2012) 40–43;
(b) Alzheimer's Disease International. World Alzheimer Report 2015. < http://www.alz.co.uk/research/WorldAlzheimerReport2015.pdf > .
(c) J. Cummings, G. Lee, T. Mortsdorf, A. Ritter, K. Zhong. Alzheimer Dement (N Y).3 (3), 367–384.
(d) < https://www.alz.org/national/documents/topicsheet_treatements.pdf > .
[2] (a) K. Beyreuther, C.L. Masters, Brain Pathol. 1 (1991) 241–251;
(b) J. Hardy, D. Allsop, Trends Pharmacol. Sci. 12 (1991) 383–388;
(c) D.J. Selkoe, Neuron 6 (1991) 487–498;
(d) J.A. Hardy, G.A. Higgins, Science 256 (1992) 184–185;
(e) D.J. Selkoe, J. Hardy, EMBO Mol. Med. 8 (2016) 595–608;
(f) R. Vassar, Alzheimer's Res. Ther. 6 (2014) 89;
(g) R. Vassar, P.H. Kuhn, C. Haass, M.E. Kennedy, L. Rajendran, P.C. Wong, S.F. Lichtenthaler, J. Neurochem. 130 (2014) 4–28.
[3] a(a) S. Filser, S.V. Ovsepian, M. Masana, L. Brazquez-Lorca, A. Brandt Elvanq, C. Volbracht, M.B. Muller, C.K. Jung, J. Herms, Biol. Psychiatry. 77 (2015) 729–739;
(b) K. Zhu, X. Xiang, S. Filser, P. Marinkovic, M.M. Dorokstar, S. Crux, U. Neumann, D.R. Shimshek, G. Rammes, C. Haass, S.F. Lichtenthaler, J.M. Gunnersen, J. Herms, Biol. Psychiatry 83 (2018) 428–437.
[4] a) (S. Merck. Merck Announces Discontinuation of APECS Study Evaluating Verubecestat (MK-8931) for the Treatment of People with Prodromal Alzheimer's Disease, 2018. Available online at: < http://investors.merck.com/news/ press-release-details/2018/Merck-Announces-Discontinuation-of-APECSStudy-Evaluating-Verubecestat-MK-8931-for-the-Treatment-of-Peoplewith-Prodromal-Alzheimers-Disease/default.aspx > (accessed February 25, 2018).
b) (E. Malone. Scrip, 2018 June;12.
(c) Jansenn. Update on Janssen's BACE inhibitor program. Titusville, United States: Company press release; 2018 May 17.
(d) < https://www.eisai.com/news/2018/pdf/enews201886pdf.pdf (accessed October 18, 2018).
(e) U. Neumann, M. Ufer, L.H. Jacobson, M.L. Rouzade-Dominguez, G. Huledal, C. Kolly, R.M. Lüönd, R. Machauer, S.J. Veenstra, K. Hurth, H. Rueeger, M. Tintelnot-Blomley, M. Staufenbiel, D.R. Shimshek, L. Perrot, W. Frieauff, V. Dubost, H. Schiller, B. Vogg, K. Beltz, A. Avrameas, S. Kretz, N. Pezous, J.M. Rondeau, N. Beckmann, A. Hartmann, S. Vormfelde, O.J. David, B. Galli, R. Ramos, A. Graf, C. Lopez Lopez, EMBO Mol. Med. (2018) pii: e9316 (November 2018);
(f) C. Lopez Lopez, A. Caputo, F. Liu, M.E. Riviere, M.L. Rouzade-Dominguez, R.G. Thomas, J.B. Langbaum, R. Lenz, E.M. Reiman, A. Graf, P.N. Tariot, J. Prev Alzheimers Dis. 4 (2017) 242–246;
(g) < http://www.ctad-alzheimer.com/files/files/CTAD%2011th%20Final%20Program%20-%2017%20oct%20BD-1.pdf > (OC-3, 11th Clinical Trials on Alzheimer's Disease Conference (CTAD), October 25, 2018).
[5] D. Kuhnke, G. Jedlitschky, M. Grube, M. Krohn, M. Jucker, I. Mosyagin, I. Cascorbi, L.C. Walker, H.K. Kroemer, R.W. Warzok, S. Vogelgesang, Brain Pathol. 17 (4) (2011) 347–353.
[6] E. Zanforlin, G. Zagotto, G. Ribaudo, Curr. Med. Chem. 24 (34) (2017) 3749–3773.
[7] (a) S.S. Lim, S. Han, S.Y. Kim, Y.E. Bae, I.J. Kang, Food Sci. Biotech. 16 (2007) 265;
(b) M. Jung, M. Park, Molecules 12 (2007) 2130;
(c) H. Kim, B.S. Park, K.G. Lee, C.Y. Choi, S.S. Yang, Y.H. Kim, S.E. Lee, J. Agric, Food Chem. 53 (2005) 8537;
(d) J. Zhu, R. Choi, G. Chu, A. Cheung, Q. Gao, J. Li, Z.Y. Jiang, T. Dong, K. Tsim, J. Agric. Food Chem. 55 (2007) 2438.
[8] (a) K. Youn, J.-H. Park, J. Lee, W.-S. Jeong, C.-T. Ho, M. Jun, Nutrients 8 (2016) 637;
(b) K. Youn, J.-H. Park, S. Lee, S. Lee, J. Lee, E.-Y. Yun, W.-S. Jeong, M. Jun, J. Med. Food. 00 (2018) 1–5.
[9] G Ribaudo, M.A. Pagano, V. Pavan, M. Redaelli, M. Zorzan, R. Pezzani, C. Mucignat-Caretta, T. Vendrame, S. Bova, G. Zagotto, Fitoterapia. 105, 132–138.
[10] (a) D. Zhao, C. Zhao, X. Chen, H. Xia, L. Zhang, H. Liu, X. Jiang, Y. Dai, J. Liu, Neurochem. Res. (2013) 2105–2113;
(b) N.H. Mohamed, H.M. Ali, M.Z.M. Salem, J. Pure Appl. Microbiol. 8 (2014) 2969–2974;
(c) H.I. Moon, Nat. Prod. Commun. 9 (2014) 1723–1724.
[11] E. Kupeli, I. Orhan, G.Toker, E. Yesilada, J. Ethnopharmacol. 107 169–174.
[12] a) G. Delle Monache, R. Scurria, A. Vitali, B. Botta, B. Monacelli, G. Pasqua, C. Palocci, E. Cernia, Phytochemistry 37 (1994) 893–898;
(b) G. Ribaudo, T. Vendrame, S. Bova, Nat. Prod. Res. (2017) 1988–1994.
[13] M.L. Wolfrom, F.L. Benton, A.S. Gregory, W.W. Hess, J.E. Mahan, P.W. Morgan, J.

Am. Chem. Soc. 61 (10) (1939) 2832–2836.
[14] Y. Hamada, H. Ohta, N. Miyamoto, R. Yamaguvhi, A. Yamani, K. Hidaka, T. Kimura, K. Saito, Y. Hayashi, S. Ishiurac, Y. Kisoa, Bioorg. Med. Chem. Lett. 18 (5) (2008) 1643–1647.
[15] L.A. Mohammed, J.N. Keller, A. Kaddoumi, Biochim. Biophys Acta 1862 (4) (2016) 778–787.
[16] M. Contino, M. Cantore, E. Capparelli, M.G. Perrone, M. Niso, C. Inglese, F. Berardi, M. Leopoldo, R. Perrone, N.A. Colabufo, ChemMedChem. 7 (2012) 391–395.
[17] V. K. Wong, Y. K. Law, T.Efferth, O. Kadioglu, L. Liu. AU Patent 101721, 2015.
[18] C. Martin, G. Berridge, C.F. Higgins, R. Callaghan, Br. J. Pharmacol. 122 (1997) 765–771.
[19] N. Colabufo, F. Berardi, M.G. Perrone, E. Capparelli, M. Cantore, C. Inglese, R. Perrone, Curr. Top. Med. Chem. 10 (2010) 1703–1714.
[20] H. Pajouhesh, G.R. Lenz, NeuroRx 2 (4) (2005) 541–553.
[21] (a) T. Suomeni, T.P. Piepponen, R. Kostianein, Plos one 10 (7) (2015) e0133904; (b) H. Asaba, K. Hosoya, H. Takanaga, S. Ohtsuki, E. Tamura, T. Takizawa, J. Neurochem. 75 (2000) 1907–1916;
(c) M. Miyajima, H. Kusuhara, M. Fujishima, Y. Adachi, Y. Sugiyama, Drug. Metab. Dispos. (2011) 814–819.
[22] (a) F.J. Rombouts, G. Tresadern, O. Delgado, C. Martinez-Lamenca, M. Van Gool, A. Garcia-Molina, S.A. Alonso de Diego, D. Oehlrich, H. Prokopcova, J.M. Alonso, N. Austin, H. Borghys, S. Van Brandt, M. Surkyn, M. De Cleyn, A. Vos, R. Alexander, G. Macdonald, D. Moechars, H. Gijsen, A. Trabanco, J. M. Chem. 58 (2015) 8216–8235;
(b) N. Maki, P. Hafkemeyer, S. Dey, J. Biol. Chem 16 (2003) 278 (20), 18132-9.
[23] V.K. Wong, T. Li, B.Y. Law, E.D. Ma, N.C. Yip, F. Michelangeli, C.K. Law, M.M. Zhang, K.Y. Lam, P.L. Chan, L. Liu, Cell Death Dis. 4 (2013) e720.
[24] M.D. Hanwell, D.E. Curtis, D.C. Lonie, T. Vandermeersch, E. Zurek, G.R. Hutchison, J. Cheminform. 4 (2012) 17.
[25] O. Trott, A.J. Olson, J. Comput. Chem. 31 (2010) 455–461.
[26] BIOvIA, D. S., Discovery studio modeling environment. San Diego, Dassault Systemes, Release, 4, 2015.
[27] Y.S. Ki, E.Y. Park, H.-W. Lee, M.S. Oh, Y.-W. Cho, Y.K. Kwon, J.H. Moon, K.-T. Lee, Biol. Pharm. Bull. 33 (6) (2010) 1054–1058.